

Supporting Information

Paper-based Mechanical Sensors Enabled by Folding and Stacking

Tong Yang¹, Jeffrey M. Mativetsky*^{1,2}

¹ Materials Science and Engineering, Binghamton University, Binghamton, NY, 13902, USA

² Department of Physics, Applied Physics, and Astronomy, Binghamton University, Binghamton, NY, 13902, USA

* Corresponding author email: jmativet@binghamton.edu

PEDOT:PSS-saturated Paper Microstructure	S-2
Pressure Sensing Devices Based on Stacked Paper Layers	S-3
Nanoscale Pressure Response	S-4
Hertz Contact Model	S-5
Folded Pressure Sensing Devices	S-6
Pressure Sensing Pixel Array	S-7
References	S-7

PEDOT:PSS-saturated Paper Microstructure

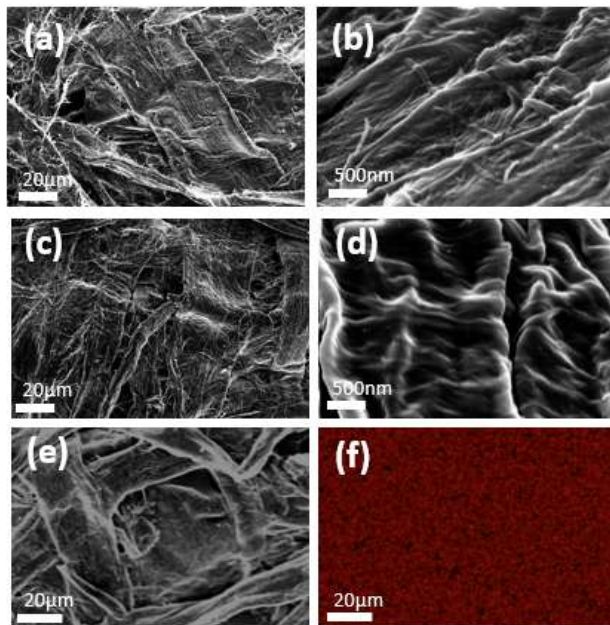


Figure S1. Scanning electron microscope (SEM) images of (a, b) tissue paper, and (c, d, e) PEDOT:PSS-saturated paper. (f) Energy-dispersive X-ray spectroscopy (EDS) sulfur map of PEDOT:PSS-saturated paper (same location as (e)), showing a quite uniform coating of sulfur-containing PEDOT:PSS on the paper fibers.

Pressure Sensing Devices Based on Stacked Paper Layers

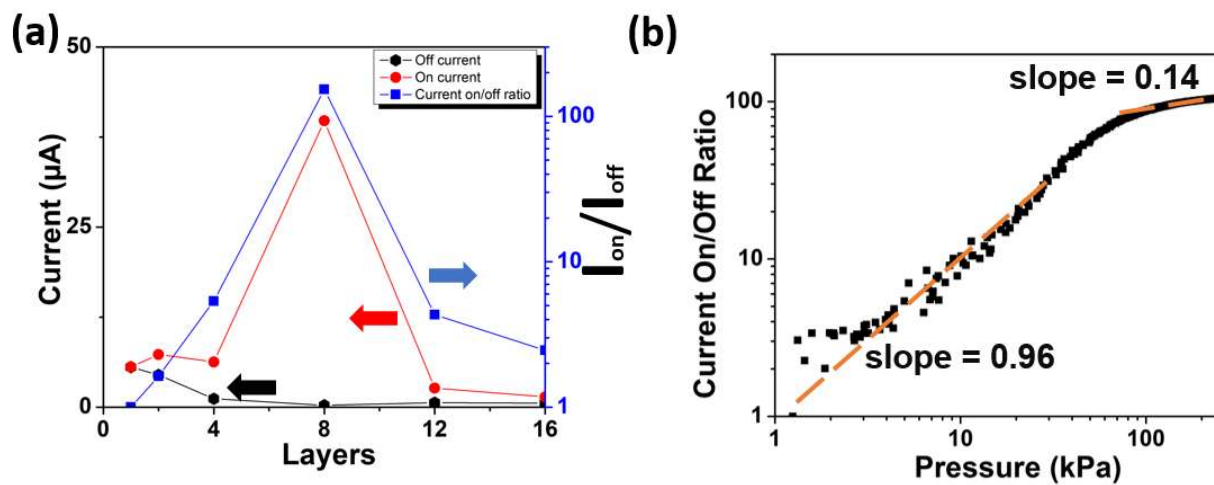


Figure S2. (a) Off current (I_{off}), on current (I_{on}), and current on/off ratio ($I_{\text{on}}/I_{\text{off}}$) for devices with varying numbers of paper layers and an applied pressure of 167 kPa. (b) Log-log plot of $I_{\text{on}}/I_{\text{off}}$ versus pressure for an 8 layer device.

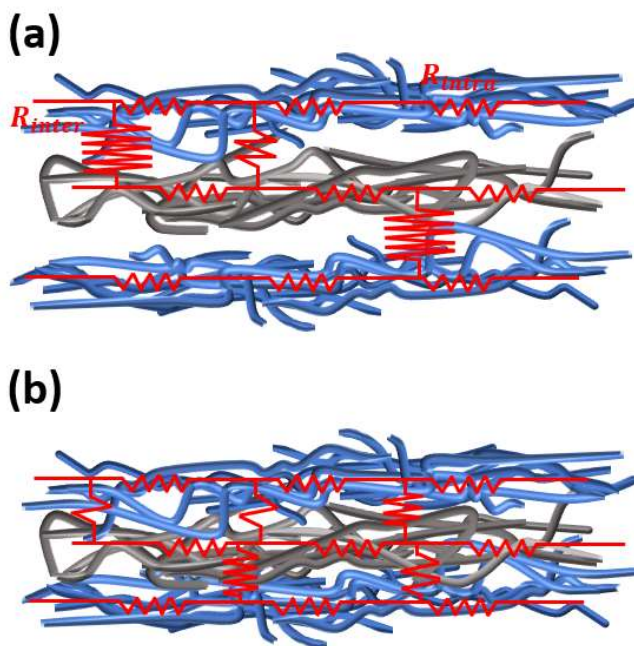


Figure S3. (a) Prior to force application, the electrical resistance between paper layers is large. (b) When force is applied, inter-sheet resistance decreases, while the intra-paper resistance remains nearly constant.

Nanoscale Pressure Response

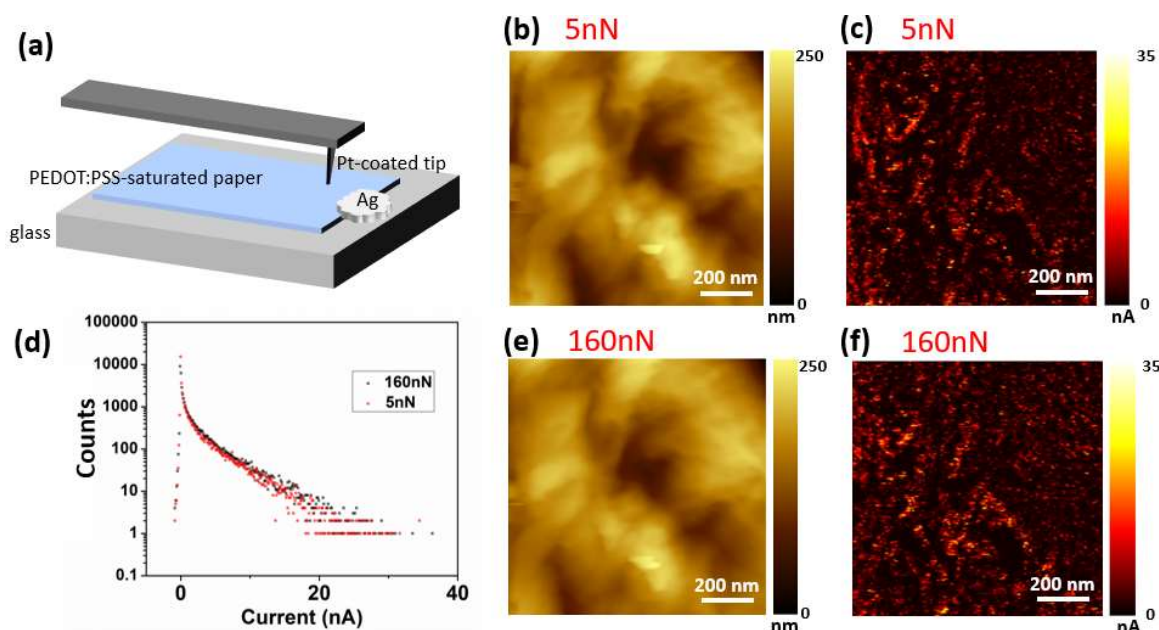


Figure S4. (a) Conductive atomic force microscope (C-AFM) setup for measuring single layer PEDOT:PSS-saturated paper. (b), (e) Topography images recorded at 5 nN and 160 nN, respectively; (c), (f) corresponding current maps showing minimal change when the force is increased to 160 nN. (d) Histogram comparing the current levels in (c) and (f).

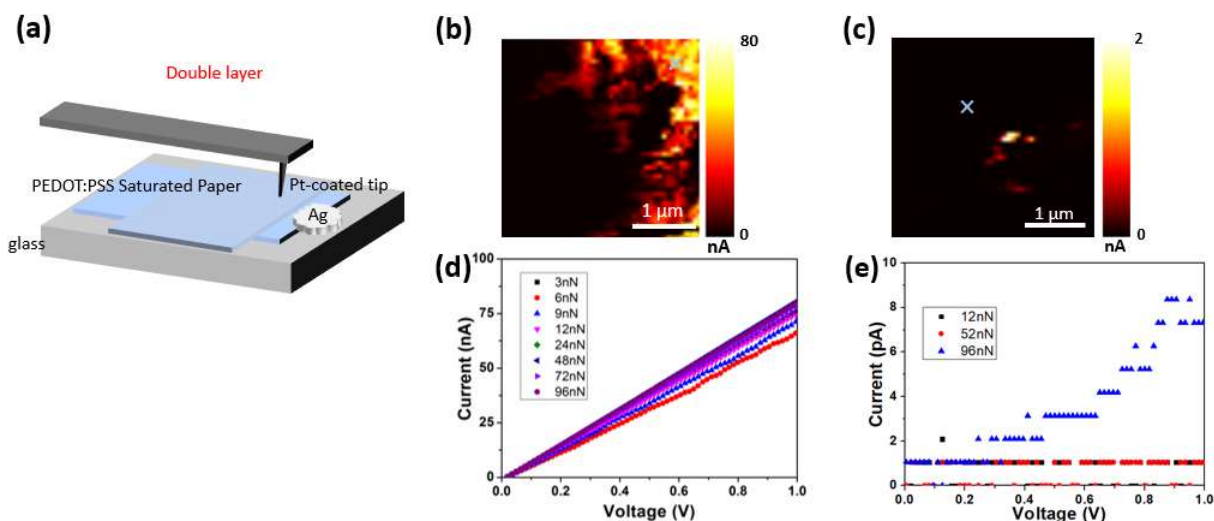


Figure S5. (a) C-AFM setup for measuring double layer PEDOT:PSS-saturated paper. (b), (c) C-AFM images at two sample regions. (d), (e) Current-voltage curves recorded at the indicated positions, showing a weak response to force (d) at a highly conductive region and (e) at a poorly conductive region.

Hertz Contact Model

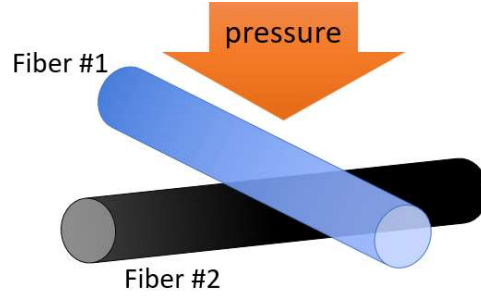


Figure S6. Schematic of two overlapping fibers being pressed into contact with one another.

When two identical cylinders of radius R and elastic modulus E come into elastic contact, as shown in Figure S6, an elliptical contact is formed. This contact geometry can be reduced to the case of a sphere in contact with a plane. The equivalent circular contact radius is given by:^{1,2}

$$c = \left(\frac{3R_c F}{4E_*} \right)^{1/3} f,$$

where F is the applied force, E_* is the contact modulus, and R_c is the radius of the equivalent sphere. The factor f is equal to or smaller than 1, and gradually decreases as the contact becomes more elliptical (i.e., when the cylinder crossing angle is less than 90°). The contact area is then given by:

$$A = \pi \left(\frac{3R_c F}{4E_*} \right)^{2/3} f^2,$$

Taking the logarithm of both sides:

$$\log(A) = 2/3 \log(F) + \text{constant}.$$

Folded Pressure Sensing Devices

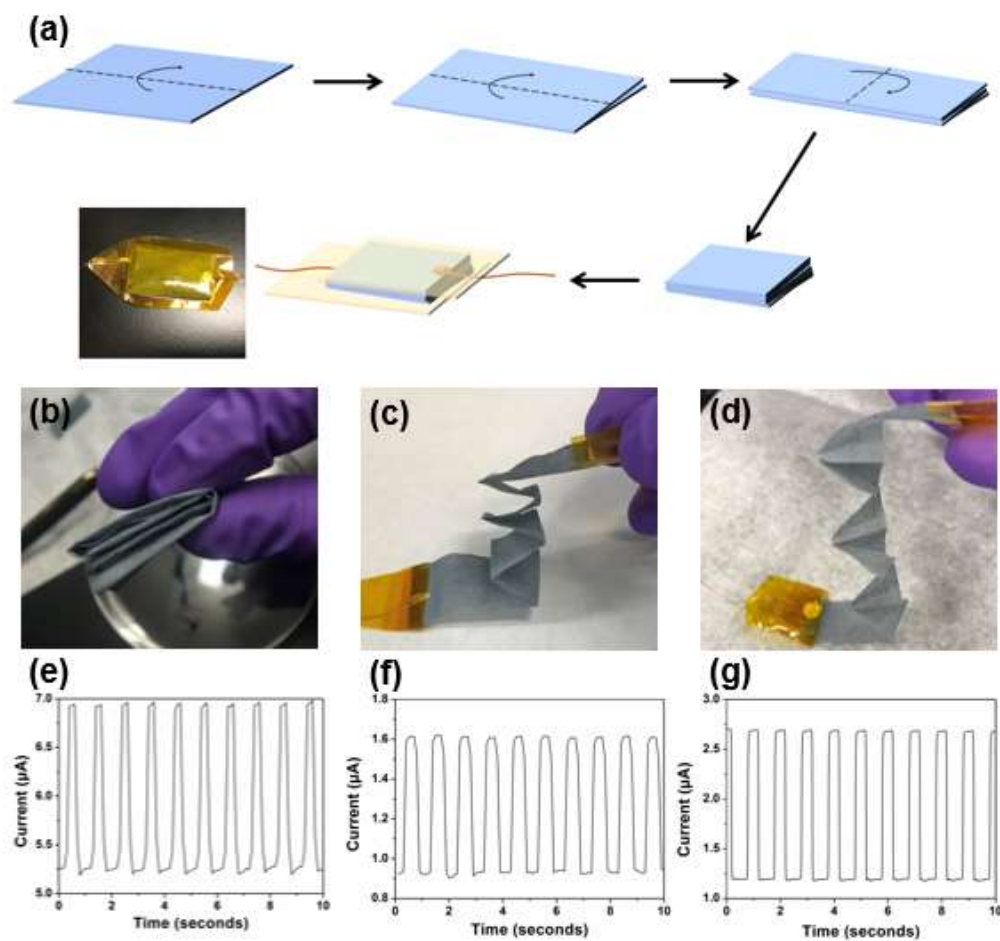


Figure S7. (a) Scheme for folding the sensor shown in (b). (c), (d) Pressure sensors made using two alternative folding geometries. (e), (f), (g) Corresponding current response to cyclic loading at 210 kPa followed by unloading.

Pressure Sensing Pixel Array

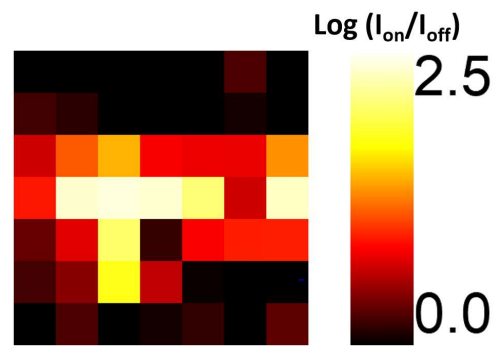


Figure S8. Raw current on-off ratio data for 7 x 7 pixel pressure sensor, without interpolation, corresponding to Figure 9c in the main text.

References

1. Johnson, K. L. *Contact Mechanics*. (Cambridge university press, 1985).
2. Bhushan, B. *Introduction to Tribology*. (John Wiley & Sons, 2013).